

A direct measure of positive feedback loop-gain due to reverse bias damage in thin-film solar cells using lock-in thermography

Suheir Nofal^{1,2,*} , Bart E. Pieters¹, Markus Hülsbeck¹, Christoph Zahren¹, Andreas Gerber¹ and Uwe Rau^{1,2}

¹ IEK5-Photovoltaik, Forschungszentrum Jülich GmbH, 52425 Jülich, Germany

² Faculty of Electrical Engineering and Information Technology, RWTH Aachen University, Mies-van-der-Rohe-Strasse 15, 52074 Aachen, Germany

Received: 30 June 2022 / Received in final form: 22 September 2022 / Accepted: 25 November 2022

Abstract. In this work, we present a method to study thermal runaway effects in thin-film solar cells. Partial shading of solar cells often leads to permanent damage to shaded cells and degrades the performance of solar modules over time. Under partial shading, the shaded cells may experience a reverse bias junction breakdown. In large-area devices such as solar cells, this junction breakdown tends to take place very locally, thus leading to very local heating and so-called “hot-spots”. Previously, it was shown that a positive feedback effect exists in Cu (In,Ga)Se₂ (CIGS) thin-film solar cells, where a highly localized power dissipation is amplified, which may lead to an unstable thermal runaway process. Furthermore, we introduced a novel characterization technique, laser induced Hot-Spot Lock-In Thermography (HS-LIT), which visualizes the positive feedback effect. In this paper, we present a modified HS-LIT technique that allows us to quantify directly a loop-gain for hot-spot formation. By quantifying the loop-gain we obtain a direct measure of how unstable a local hot-spot is, which allows the non-destructive study of hot-spot formation under various conditions and in various cells and cell types. We discuss the modified HS-LIT setup for the direct measurement of the loop-gain. Furthermore, we demonstrate the new method by measuring the loop-gain of the thermal runaway effect in a CIGS solar cell as a function of reverse bias voltage.

Keywords: Reverse bias damage / hot-spot / CIGS thin-films / thermal runaway / lock-in thermography

1 Introduction

Copper indium gallium diselenide (CIGS) solar cells technology is a promising thin film technology. As CIGS material offers high absorption coefficient for solar radiation, a very thin absorber layer is required to achieve relatively high efficiency. This advantage gives the solar cell the ability to be deposited on thin, light weight, and flexible substrates like polymers and steel. As a result CIGS modules can reach high weight specific power densities, which makes the technology interesting for e.g., aerospace and unmanned aerial vehicles (UAV), portable charging, micro-integrated products, and vehicle- and building-integrated photovoltaics [1]. However, in many integrated PV applications, the PV modules are often exposed to partial shading from the environment, e.g. trees or building structures. Partial shading is known to lead to performance degradation in CIGS [2].

Under partial shading, the shaded cells may be reverse biased and be driven into a junction breakdown. Under junction breakdown, the solar cell may become locally highly conductive. If the cell is locally much more conductive than its surroundings, it may pull in current from its surroundings leading to a high local power dissipation. Since the layer stack is thin and typical encapsulation materials are poor conductors for heat, the local generated heat cannot flow away quickly and a hot-spot is formed [3]. Such a local hot-spot may act as the seed for thermal runaway process leading to permanent damage and typically manifests itself as “wormlike damages” [3–9]. At these defects structural changes are observed in the materials, which suggest very high local temperature. The damage leads to porous material and acts like a shunt [5]. The hot spots tend to propagate through the material, leaving a trail of damage, leading to their worm-like appearance.

Recent experiments demonstrate that a positive feedback loop can trigger the formation of local hot-spots [10–12]. A positive feedback, or a loop-gain larger than 1, leads to inherently unstable processes. In case of reverse-bias

* e-mail: s.nofal@fz-juelich.de

hot-spot formation in CIGS, the identified positive feedback concerns a highly localized heat dissipation. If heat is dissipated in a small area exhibiting junction breakdown, the small area heats up, leading to an *increase* in breakdown current, which in turn increases the local power dissipation. Note that in CIGS junction breakdown is highly temperature dependent [13]. This positive feedback leads to a situation where a relatively small defect can quickly develop into a thermal runaway process.

In our previous work [3], we successfully introduce laser induced Hot-Spot Lock-In Thermography (HS-LIT) as a characterization method to investigate the formation of hot-spots in thin-film solar cell technologies and visualize the positive feedback loop. In which, we induce a local hot-spot in the solar cell and investigate the positive feedback effect due to the applied reverse bias stress. Our method allows a non-destructive investigation of the hot-spots formation, i.e. we observe the increase in temperature before the temperature reaches a critical value. Furthermore, the method shows a clear interaction between local temperature distribution and power dissipation in the cells, where a local hot-spot leads to a redistribution of the dissipated electrical power focusing most of the dissipated power in the hot-spot. In this work we introduce a slightly modified HS-LIT experiment that allows to assess a quantitative loop-gain value. The quantification of the loop-gain provides a direct measure of how unstable the hot-spot is. This allows a quantitative comparison between cells under various conditions in a non-destructive experiment.

In Section 2 we introduce our improved HS-LIT setup that is used for lock-in experiments. Our experimental results are presented and discussed in Section 3. Finally, in Section 4 we summarize the presented work.

2 Experimental

The used samples are cut from industrially semi-produced CIGS modules. The device structure consists of a ZnO/CdS/Cu(In,Ga)Se₂/Mo/Glass layer stack, where the CIGS is produced in a co-evaporation process and the CdS buffer using a chemical bath deposition [14]. Each cut module consists of 4 individual minimodules on 10 × 10 cm² glass substrate. The minimodules in turn consist of 10 series connected solar cells, each with a dimension of 0.4 × 4 cm². The cells are monolithically interconnected. We scratched every second cell and applied contact strips. This way we obtain individually contacted cells for our experiments. Finally, all modules are encapsulated using ethylene vinyl-acetate (EVA) layer and a polyester (PET) layer as front cover.

In our previously presented HS-LIT method we applied a Continuous Wave (CW) laser source to induce a local hot spot. The electrical excitation was modulated with the lock-in frequency [3]. The downside of this method is that the CW laser is not modulated, and thus it produces no lock-in signal. The measured electrical signal cannot be put into relation with the laser power. In our new setup we added the possibility to modulate the laser. Therefore, we can measure the LIT response with and without a DC

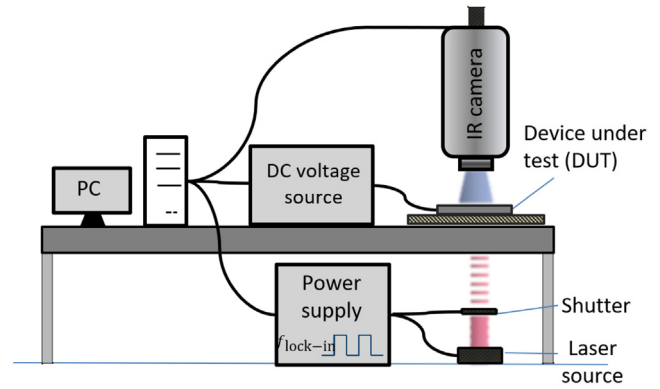


Fig. 1. Schematic image of LIT setup. The laser source is modulated using an optical shutter. The reversed biased voltage is applied in its DC state.

electrical bias. This way we can compute a loop-gain by dividing the LIT response with and without the DC electrical excitation. The setup is illustrated in Figure 1. We use a Heubner GmbH diode Infra-Red (IR) laser source with a wavelength of 1064 nm. The maximum power of the laser is 2.0 W. In a dark cabinet at room temperature 20 °C, the laser is being directed to the backside of the device under test (DUT). As our samples are on a glass substrate the laser is incident through the glass on the molybdenum layer, and locally heats the molybdenum, and the CIGS above it. It is important to note here that we observe no photocurrent, i.e. the molybdenum is opaque to the laser and no noticeable stray laser light irradiates the solar cell. The laser power can be adjusted using a half wave plate and modulated using an optical shutter. We use an automatic actuator with an of LMH-1064-20X high-power micro-spot focusing objective lens to change the laser beam size. However, we use the laser beam in-focus with the minimum diameter of 5 μm. All these optical components are from THORLABS GmbH.

The thermal camera is an imageIR 9300 from InfraTec GmbH. The camera uses an InSb detector, and is sensitive to wavelengths between 2.0 and 5.7 μm. The resolution is 1280 × 1024. For this work, we use a laser power of 50 mW. To produce Lock-in amplitude images, the InfraTec GmbH “IRBIS Active Online” software is used. In which, we use a duty cycle of 50%. The shutter receives the lock-in frequency from the camera at 0.50 Hz. The measurement is acquired over 100 periods, from which the first two periods are dropped to reject the initial transients. The framerate of the camera is set to 40 frames/period. We measured the emissivity of the encapsulation layers in the relevant spectral range using Fourier-transform infrared spectroscopy. The emissivity was determined to be around 0.96. All intensities are corrected for the emissivity.

Meanwhile, we apply the DC voltage excitation in reverse and record the electrical response using a Keithley source measuring unit (SMU 2425). The electrical characteristics of the cells under investigation are measured by a dark IV sweep that covers a voltage range between −0.20 V and +1.20 V before and after each experiment using the same SMU2425.

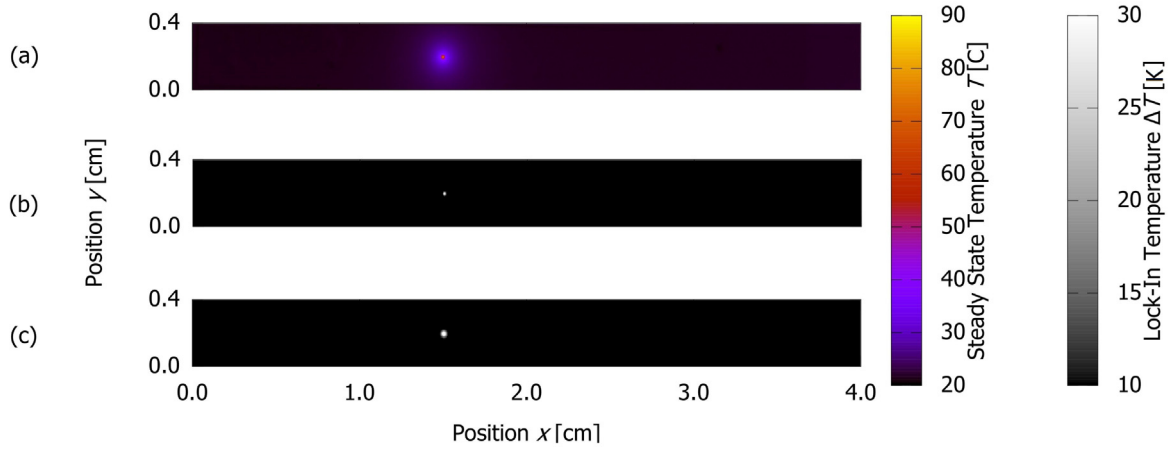


Fig. 2. Results of lock-in measurements using the updated setup. (a) Steady state thermographic image; (b) Lock-in image of a sample when only the modulated laser is applied; (c) Lock-in image of the sample when the modulated laser with a DC reversed voltage are applied simultaneously.

3 Results and discussion

3.1 LIT analysis

In our experiment, the stimulus signal $E(t)$ represented as the modulated laser is applied to the DUT (with or without a DC voltage) with a specific lock-in frequency ($f_{\text{lock-in}}$ of 0.50 Hz). The stimulus E will cause a thermal response of the DUT that would be detected by the thermal camera. This measured response signal $F(t)$ is a noisy signal. Hence, to detect the beneficial lock-in response signal of the system (S) without noise [15,16], the following equation is used:

$$S = \frac{1}{t_{\text{int}}} \int_0^{t_{\text{int}}} F(t)K(t)dt \quad (1)$$

where t_{int} is the integration time which represent the time of the measurement, and $K(t)$ is the symmetric square wave correlation factor, calculated as:

$$K(t) = \begin{cases} +2 & \text{for } 0 \leq t < \frac{T}{2} \text{ within one period } T \\ -2 & \text{for } \frac{T}{2} \leq t < T \text{ within one period } T \end{cases} \quad (2)$$

A digital amplifier is normally used for the lock-in analysis, where the noisy signal is digitized into series of F_j and K_j . Hence, the integral from equation (1) yields the sum as follows

$$S = \frac{1}{nN} \sum_{i=1}^N \sum_{j=1}^n K_j F_{i,j} \quad (3)$$

where N is the number of lock-in periods (100 periods), and n is the number of frames within one period (40 frames/period). This would mean that each measurement has $n \times N$ number of images or frames that are averaged. The

frames in each lock-in period are then weighted by the weighting factors $K_j^{0^\circ}$ and $K_j^{90^\circ}$ which represent sine and cosine functions, respectively:

$$K_j^{0^\circ} = +2 \frac{\sin(2\pi(j-1))}{n}, \quad (4)$$

$$K_j^{90^\circ} = -2 \frac{\cos(2\pi(j-1))}{n} \quad (5)$$

where 0° and 90° are the primary phase shifts of a LIT measurement. The phase shift at 0° represent the heat diffusion in-phase to the heat introduction, while the phase shift at 90° represents the delay [15]. Therefore, two components of the signal S can be computed; including the in-phase component S^{0° with no phase shift and the quadratic component S^{90° with a phase shift of 90° , as:

$$S^{0^\circ} = \frac{1}{nN} \sum_{i=1}^N \sum_{j=1}^n K_j^{0^\circ} F_{i,j}, \quad (6)$$

$$S^{90^\circ} = \frac{1}{nN} \sum_{i=1}^N \sum_{j=1}^n K_j^{90^\circ} F_{i,j}. \quad (7)$$

Finally, the lock-in amplitude A of the beneficial response S for each measurement is calculated by:

$$A = \sqrt{(S^{0^\circ})^2 + (S^{90^\circ})^2}. \quad (8)$$

3.2 Loop-gain

From IRBIS Active Online, we have taken two types of images; steady state and lock-in amplitude images. Figure 2a, shows the steady state thermographic image from the thermal camera. For the steady state image we use

the absolute temperature color scale. Meanwhile, Figures 2b and 2c present the lock-in amplitude images, which use the shown differential temperature amplitude gray scale.

In the first experiment, only the modulated laser is applied to the sample. The steady state image in Figure 2a shows the laser induced hot-spot in the device. The corresponding lock-in image in Figure 2b shows a clear signal in the location of the hot-spot since the laser is modulated. The spot has a maximum lock-in amplitude of 38.295 K.

We have repeated the same experiment on the same sample but with an additional DC reversed voltage of 3 V. As observed in Figure 2c, the corresponding lock-in image shows a higher thermal response. The spot now has a maximum lock-in amplitude of 63.873 K. Furthermore, the size of the hot-spot is notably larger. Since the applied voltage is in its DC state, this increase in the thermal response is due to the interaction between the modulated laser induced hot-spot and the applied biased voltage. The hot-spot leads to a redistribution of the dissipated power where most of it is focused in the local hot-spot. Hence, the modulation in hot-spot temperature leads to a modulation of the local electrically dissipated power.

We define the local hot-spot loop-gain (g_L) as the ratio between the lock-in amplitude with and without electrical excitation.

$$g_L = \frac{A_{1e}}{A_1} \quad (9)$$

where, A_{1e} is the amplitude with modulated laser *and* DC electrical excitation, and A_1 with modulated laser only.

As the size and shape of the hot-spot may be different, we define the overall loop-gain as

$$G_L = \frac{\iint_{\Omega} A_{1e} d\Omega}{\iint_{\Omega} A_1 d\Omega} \quad (10)$$

where, Ω denotes the cell area within the lock-in amplitude images. In our experiment shown in Figure 2, the overall loop-gain of the hot-spot reaches 2.03 and the maximum local loop-gain equals 1.67.

In case the loop-gain is larger than one, we speak of a positive feedback. When a system exhibits a positive feedback, any small perturbation in the system is amplified, and thus, such systems are inherently unstable and chaotic (chaotic as all small perturbations may have large implications). In the context of our experiment, a positive feedback potentially leads to a thermal runaway. It is important to note that our definition of loop-gain is based on lock-in amplitudes, and thus, we only measure the loop-gain at one specific frequency. Furthermore, the lock-in experiment measures a steady-state response, i.e. the system as it is measured is *not* unstable *despite* the loop-gain larger than one. The measurement thus tells us that under DC conditions the system would be unstable and a thermal runaway would be triggered. In other words, the thermal mass of the system effectively imposes a low pass

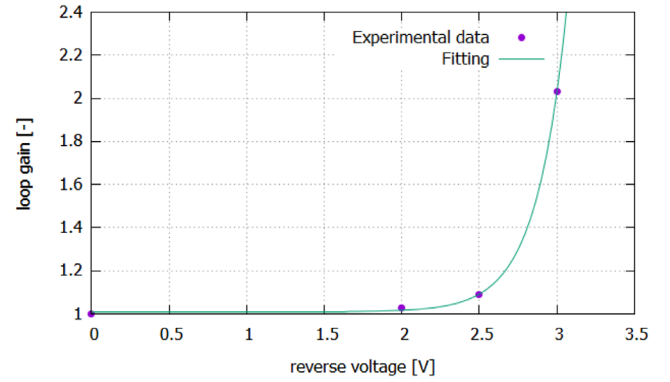


Fig. 3. Loop-gain as a function of reverse voltage. Loop-gain is increasing exponentially w.r.t the applied reverse biased voltage.

filter¹ to the thermal response of the system. Due to this low-pass filter the overall system response to the excitation is limited to levels where the system remains stable.

If we consider the measured loop-gain of 2.03 in the hot-spot, it implies an amount of dissipated heat in the hot-spot is amplified 2.03 times within the 1 second "on-period" of one lock-in period (the laser is modulated at 0.5 Hz with a 50% duty cycle). Thus the implied temperature rise under DC conditions is exponential with a doubling of the temperature every second. It must be stressed that this loop gain is obtained at the specific conditions of the measurement, i.e. under DC conditions it is to be expected the loop gain will change over time as the hot spot gets hotter and bigger. However, the measured loop gain of 2.03 does constitute a massive instability, which is likely to cause a thermal runaway and irreversible damage to the sample in a short period of time.

We repeated the HS-LIT experiments on the same cell, where we varied the DC reverse voltage, whilst all other experimental parameters are kept the same. The overall loop-gain for these experiments are presented in Figure 3. The results show a highly super linear loop-gain with the reverse bias voltage. The line in Figure 3 is an exponential fit, which we add as a guide to the eye. Attempts to measure the response to higher reverse bias voltages resulted in the destruction of the sample.

3.3 Discussion

As in our experiment we measure a lock-in response of the system to the laser and electrical power, we can relate the measured electrical power to the absorbed laser power. In the following we verify the consistency of our measurement by comparing the measured electrical response and the laser power, i.e. we check whether we can account for all the modulated heat in the system. From the measured electrical power we can compute the lock-in amplitude. The 0° and 90° lock-in signals (F^{0° and F^{90° , respectively) equal

$$F^{0^\circ} = 2P(t)\sin(2\pi ft), \quad (11)$$

$$F^{90^\circ} = 2P(t)\cos(2\pi ft) \quad (12)$$

¹ The thermal capacitance combined with thermal conductivity of the material form a low pass filter for heat.

where t is the time, and $P(t)$ is the measured injected electrical power. The electrical power amplitude (A_{Pe}) then equals

$$A_{Pe} = \sqrt{(F^{0^\circ})^2 + (F^{90^\circ})^2}. \quad (13)$$

Likewise, we may define the laser power amplitude (A_{Pl}) as the lock in amplitude of the absorbed laser power. The laser power is modulated as a square wave with a duty cycle of 50%. For the absorbed laser power we can write

$$P_1 = P_{0,1} \alpha \operatorname{sgn}(\sin(2\pi ft)) \quad (14)$$

where, α is the absorbance of the laser in the molybdenum, $P_{0,1}$ the incident laser power and sgn is the sign function (i.e. $\operatorname{sgn}(\sin(2\pi ft))$ is a square wave. Applying equations (11), (12), and (13) to equation (14), we obtain

$$A_{Pl} \approx P_{0,1} \alpha (1.2719) \quad (15)$$

where we computed the amplitude of the unit square wave with the parameters for the experiment, namely 40 samples per period (the same as the number of frames per period). The value of 1.2719 is close to the theoretical $4/\pi \approx 1.2732$, which is the amplitude of the ground frequency of a square wave.

Before, we computed the loop-gain from the integral thermographic response. The same loop-gain should also apply to the injected laser and electrical power, and thus

$$A_{Pl} = \frac{A_{Pe}}{G_L - 1}. \quad (16)$$

For the electrical power amplitude during the experiment we find $A_{Pe} = 16.4$ mW, and for the gain we had $G_L = 2.03$. Thus, using equation (16) we find $A_{Pl} = 15.92$ mW. The laser power was set to 50 mW. However we have optical losses in the half-wave plate, which reduces the incident laser power to $P_{0,1} = 43$ mW. We thus can compute the absorbance of the laser as $A_{Pl}/(1.2719P_{0,1}) = 0.29$. For comparison we can compute how much absorbance we would expect for a laser with wavelength 1064 nm incident on a Air/Glass/Mo optical system. To this end we assume a refractive index of glass of 1.5. For the molybdenum we assume a complex refractive index of $n_{Mo}^* = 2.3016 + 4.4153i$ [17]. From this we obtain an absorbance of $\lambda = 0.25$. The deviation between the computed and the theoretical absorbance is likely due to different optical properties of the Glass/Mo interface.

4 Conclusions

We presented a HS-LIT method by which we can quantify the loop-gain for hot-spot formation in CIGS solar cells. It is argued that the loop-gain value is a measure of how fast a thermal runaway develops under certain conditions. We have shown that using lock-in we may quantify a loop-gain in excess of 1 without permanently damaging the sample. We achieve this by measuring the loop-gain at the lock-in frequency under conditions that the system *would* be

unstable under DC conditions. We have shown experimental loop-gain values for industrially produced CIGS cells of up to 2.03, at a reverse bias of 3 V. Furthermore, we show the loop-gain is highly super linear, making the sample more prone to thermal runaway processes at higher reverse bias voltages. As a consistency check we verified the results obtained in the thermographic lock-in images is consistent with the overall electrically and optically injected power during the experiments.

This work was partially supported by the German Federal Ministry of Education and Research (BMBF: Funding reference number 01DH16027) within the framework of the Palestinian-German Science Bridge project, the Reliability Lab project (325-8.04.08.06) funded by the Ministry of Culture and Science of the State of North Rhine-Westphalia MKW, and the OptiCIGSII project (FK0324297D) funded by the Federal Ministry of Economics and Technology BMWK.

Author contribution statement

B.P and U.R conceptualized the idea. S.N. conducted the Experimental work and analyzed the data. M.H. and C.Z. helped realizing the experimental setup. B.P. and A.G. supervised the work.

References

1. M.O. Reese, S. Glynn, M.D. Kempe, D.L. McGott, M.S. Dabney, T.M. Barnes, S. Booth, D. Feldman, N.M. Haegel, *Nat. Energy* **3**, 1002 (2018)
2. K. Bakker, A. Weeber, M. Theelen, *J. Mater. Res.* **34**, 3977 (2019)
3. S. Nofal, B.E. Pieters, A novel non-destructive characterization method to investigate hot-spot formation in CIGS solar cells using lock-in thermography, in *2021 IEEE 48th Photovoltaic Specialists Conference (PVSC)* (2021), pp. 1328–1330
4. C.G. Zimmermann, *Appl. Phys. Lett.* **102**, 233506 (2013)
5. P.O. Westin, U. Zimmermann, L. Stolt, M. Edoff, *Reverse Bias Damage in CIGS Modules in 24th European Photovoltaic Solar Energy Conference and Exhibition* (2009), pp. 2967–2970
6. E. Palmiotti, S. Johnston, A. Gerber, H. Guthrey, A. Rockett, L. Mansfield, T.J. Silverman, M. Al-Jassim, *Sol. Energy* **161**, 1 (2018)
7. S. Johnston, D. Sulas, E. Palmiotti, A. Gerber, H. Guthrey, J. Liu, L. Mansfield, T.J. Silverman, A. Rockett, M. Al-Jassim, *Thin-Film Module Reverse-Bias Breakdown Sites Identified by Thermal Imaging*, in *2018 IEEE 7th World Conference on Photovoltaic Energy Conversion (WCPEC) (A Joint Conference of 45th IEEE PVSC, 28th PVSEC 34th EU PVSEC)* (2018), pp. 1897–1901
8. O. Breitenstein, J. Bauer, K. Bothe, W. Kwapil, D. Lausch, U. Rau, J. Schmidt, M. Schneemann, M.C. Schubert, J.M. Wagner et al., *J. Appl. Phys.* **109**, 071101 (2011)
9. K. Bakker, H.N. Ahman, T. Burgers, N. Barreau, A. Weeber, M. Theelen, *Sol. Energy Mater. Sol. Cells* **205**, 110249 (2020)
10. T.S. Vaas, B.E. Pieters, U. Rau, *IEEE J. Photovolt.* (submitted)
11. V. Karpov, *Phys. Rev. B* **86**, 165317 (2012)

12. M. Nardone, S. Dahal, J. Waddle, Sol. Energy **139**, 381 (2016)
13. T.J. Silverman, M.G. Deceglie, X. Sun, R.L. Garris, M.A. Alam, C. Deline, S. Kurtz, IEEE J. Photovolt. **5**, 1742 (2015)
14. B. Dimmler, R. Wächter, Thin Solid Films **515**, 5973 (2007)
15. O. Breitenstein, J.P. Rakotoniaina, M. Kaes, S. Seren, T. Pernau, G. Hahn, W. Warta, J. Isenberg, *Lock-in Thermography: a universal tool for local analysis of solar cells* (2005)
16. B. Misic, U. Rau, J. Werner, *Analysis and Simulation of Macroscopic Defects in Cu(In,Ga)Se₂ Photovoltaic Thin Film Modules* (Universitätsbibliothek der RWTH Aachen, 2015)
17. M.A. Ordal, R.J. Bell, R.W. Alexander, L.A. Newquist, M.R. Querry, Appl. Opt. **27**, 1203 (1988)

Cite this article as: Suheir Nofal, Bart E. Pieters, Markus Hülsbeck, Christoph Zahren, Andreas Gerber, Uwe Rau, A direct measure of positive feedback loop-gain due to reverse bias damage in thin-film solar cells using lock-in thermography, EPJ Photovoltaics **14**, 3 (2023)